Article

Implementation of Driving Cycles Based on Driving Style Characteristics of Autonomous Vehicles

Xucheng Duan *, Ferdinand Schockenhoff and Alexander Koch

Institute of Automotive Technology, TUM School of Engineering and Design, Technical University of Munich, Boltzmannstraße 15, 85748 Garching, Germany; ferdinand.schockenhoff@tum.de (F.S.); alexander.koch@tum.de (A.K.)
* Correspondence: xucheng.duan@tum.de

Abstract: The standardized driving cycles, which are used around the globe for the development and homologation of automobiles, consist of a series of speed points versus time, to represent typical driving conditions and to exclude the influence of a human driver. However, with respect to autonomous vehicles (AVs), the driving style is defined in driving algorithms as a characteristic of the vehicle. Therefore, driving style should be considered in driving cycles. In this research, using MATLAB/Simulink® we developed the AVDC (Autonomous Vehicle Driving Cycle) Tool, which is capable of generating driving cycles based on driving style characteristics. The autonomous vehicles being investigated drive in a simulated environment along a straight road amongst other traffic vehicles, applying standard cycles to ensure the representativeness of generated autonomous cycles. The autonomous vehicle is piloted by adaptive cruise control (ACC) for car-following and free driving. Overtake logic decides whether passing will be attempted. Driving style is defined by four aspects—comfort, safety, swiftness, and economy—and determines the control parameters in the driving algorithm. The driving cycles generated by the AVDC Tool for a variety of driving styles show diverse characteristics, thus indicating the effective representation of various driving styles.

Keywords: driving cycle; driving style; autonomous vehicle

1. Introduction

Nowadays, autonomous driving is a significant trend in the automotive industry [1–3]. Numerous automotive manufacturers, suppliers, start-ups, and research institutes are conducting research and development on relevant technologies including algorithms. Autonomous vehicles change the relationship between human and vehicle as the driver is no longer required, and every person inside the vehicle is a passenger. As a result, the design concept for vehicles should be adapted to improve user experience during autonomous driving situations [4]. Automotive manufacturers should develop AVs in such a way that users can comfortably perform numerous activities during the trip, such as reading, watching videos, playing, and working.

In the current development of vehicles, driving cycles are commonly used to evaluate the consumption and emissions of traditional vehicles [5], or the range of electric vehicles, as well as to iteratively optimize technical design [6,7]. The current driving cycles all have fixed speed profiles in order to eliminate driver influence [8]. However, in AVs the driving style is a feature of the vehicle itself. Therefore, it should be considered in the driving cycles. In this context, we focus on designing driving cycles for AVs that depend on the driving style.

With this aim, the AVDC (Autonomous Vehicle Driving Cycle) Tool [9] was developed using MATLAB/Simulink® [10], which utilizes a specific driving style as an input when generating a cycle. Therefore, a driving cycle can be constructed for a certain driving style. The driving style is divided into four aspects within the tool: comfort, safety, swiftness, and economy. In the simulation, the AV being investigated followed a configurable scenario

in which it drove among traffic vehicles on a straight road. The chosen driving style determined the control parameters of the driving algorithm. The simulated speed profile of the AV was recorded as the output cycle.

2. State of the Art

The objective of this research—driving cycles for AVs—is a new topic addressed in few publications, although partially automated (SAE Level 2 [11]) vehicles are already running on public roads. Therefore, papers from the relevant research fields will be reviewed in this section, namely driving cycle, driving style, and AV assessment.

2.1. Development of Driving Cycles

Extensive studies are being conducted on the development of driving cycles, based on which numerous cycles have been created in various countries and regions [12]. Examples of existing driving cycles used in legislative regulations for passenger cars include the New European Driving Cycle (NEDC) [5], the Worldwide harmonized Light vehicles Test Cycle (WLTC) [13], FTP 75 (Federal Test Procedure) [12] in the USA, the China Automotive Test Cycle (CATC) [14], and JC08 (Japan Cycle) [15] in Japan. A comprehensive collection of existing driving cycles can be found in [8,16].

Galgamuwa et al. [17] summarized the methods used in the literature regarding driving cycle development and divided the procedure into four steps: route selection, data collection, cycle design, and cycle evaluation. Real-world driving data on the selected routes are first collected and processed. Then, a driving cycle is generated and evaluated based on the data, in order to statistically represent real driving conditions. Figure 1 shows the general procedure for driving cycle development using driving data.
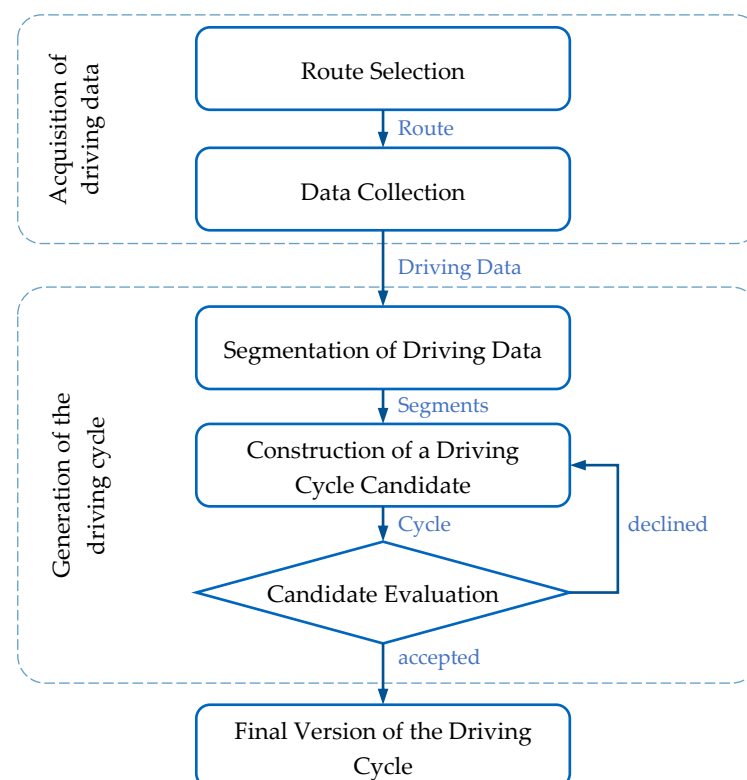

Figure 1. General procedure for driving cycle development using real driving data, based on [16,18].

The existing approaches were designed for vehicles driven by humans, since cycle construction using real-world driving data ensures a good representability of vehicle usage. For AVs, a similar approach can be adapted using AV driving data. Nevertheless, individual

driving style is not considered in this method, which fails to meet the objective of this research. Our new method will be explained in Section 3.

2.2. Evaluation of Driving Style

As a subjective and empirical concept, driving style has no standard definition and is described variously in the literature. Elander et al. [19] offered the following definition: Driving style refers to "the way individuals choose to drive, or driving habits that have been established over a period of years". Sagberg et al. [20] reviewed definitions within articles and found three common points: First, driving styles differ from person to person or between groups of people. Second, a driving style is a habitual manner of driving that represents a relatively stable aspect of driving behavior. Third, in most definitions, driving styles reflect conscious decisions by the driver. Several factors could influence the driving style of a driver—including personality, driving experience, driving knowledge, driving environment, social culture, and technical aspects [20,21].

The influence of driving style exists on a variety of levels. In terms of traffic engineering, the driving style of vehicles influences traffic flow density [22,23] and road safety [20]. At the vehicle level, energy consumption and emissions are influenced by driving style [24–26]. For passengers, driving style affects travel comfort and safety [27–29].

The research on driving style can be divided into two categories—classification and valuation. In the former category, driving styles have been classified in several types. A typical classification is based on whether the driver drives fast, which then leads to two or three classes: A driver with a fast driving style, also referred as aggressive [30,31], sporty [32], or assertive [33], prefers high speed, high acceleration, and a short distance from the vehicle ahead. A driver with a slow driving style, also called cautious [30], comfortable [32,34], calm [31], or defensive [33], prefers the opposite. The third class refers to the style in between, i.e., normal.

In the valuation category, the examined driving styles are assessed with a numeric score. Therefore, the driving style can be evaluated for various aspects. Jachimczyk et al. [35] chose eight indicators for the rating of three driving style aspects—comfort, safety, and economy. Each indicator (based on the examined driver) is first scaled with an expert value into a rating from 0 to 1. The ratings for the same aspect are combined into an overall aspect rating using the area enclosed by all relevant ratings. Numerous research projects focus on a specific aspect rather than overall driving style. Schockenhoff et al. [34] studied ride comfort during two driving maneuvers—double 90° turn and slalom. The test subjects sat in the test car while the maneuvers were being performed with specific driving styles. The relationships between the subjects' ratings of discomfort and the data for measured indicators were evaluated using regression analysis. Regarding subjective feeling of safety, Kondoh et al. [36] studied driver risk perception during car-following on a driving simulator. Two indicators were selected: time-to-collision (TTC) and time-headway (THW). The overall risk perception (RP) was defined as the weighted sum of their reciprocals. Lu et al. [37,38] pointed out the limitations of RP and proposed another valuation for safety—the safety margin (SM) value, which considers reaction time and maximum deceleration during braking. The SM corresponds to subjective safety better than RP in wider speed ranges.

The main issue for driving style evaluation is that of choosing appropriate criteria and indicators. Several researchers have investigated driving style during certain maneuvers, including car-following on a motorway [23,30], overtaking on a motorway [39], braking to a full stop [40], lane changing [34], and slalom [34]. During the maneuvers, related physical values were measured and used directly or indirectly as indicators of driving style. Another option is that of evaluating the driving style for a whole trip. In this case, average and root mean square (RMS) values have been used for indicators. Typically measured values include velocity, acceleration, distance, and time-headway to the front vehicle [31,35,41]. These values are feasible and could indicate several aspects of driving style.

2.3. Assessment Methods for Autonomous Vehicles

With conventional vehicles, driving cycles are used to benchmark energy consumption and emissions. In the evaluation of electrical vehicles, driving cycles are also important for range determination. Although autonomous driving has been researched in numerous studies, there exist few publications about the assessment methods.

Mersky and Samaras [42] developed a test procedure for AV consumption. In the simulation, the tested AV follows a vehicle applying the American legislative driving cycle (FTP or HWFET). Initially, the test vehicle is positioned 5 m behind the front vehicle before the latter starts moving. The AV follows using an ACC (Adaptive Cruise Control) system. The test ends when the front vehicle completes its driving cycle. The speed profile of the AV is recorded as the cycle, based upon which the consumption during the process is calculated by means of a consumption model. Depending on various parameters in the ACC strategy, the fuel efficiency of the AV cycle can vary from 3% worse to 10% better than the original cycle.

Roshdi, et al. [43] proposed an evaluation framework for AVs that converts data from test drives or simulations into standardized test data. The series of built-in criteria, as well as user-defined criteria, can be used for the evaluation. Since this study focuses on the framework, the exact equations for calculating the criteria have been omitted.

2.4. Research Gap

As mentioned in Section 2.1, the conventional methods for driving cycle development are not suitable for AVs. Mersky and Samaras [42] proposed a method in which the AV follows a vehicle running with standard cycles, but driving style is not investigated in this method.

For AVs, the driving style is an important characteristic for customers and has yet to be thoroughly investigated (Section 2.2). Driving styles are often classified into a few types, which are insufficient for representing the variety of driving styles regarding different customers. The indicators for driving styles have been proposed in various papers.

This paper intends to fill the gap between driving style and driving cycle. We objectively represented the driving style with objective indicators and implemented the driving style when generating a driving cycle.

3. Development of the AVDC Tool

The AVDC Tool is capable of generating driving cycles based on various driving style settings. In this section, the methods for development of the tool are described in detail.

3.1. Concept

According to the defined objective, the input of the tool is the driving style. In addition, the output cycle is defined as a speed–time profile. The concept is explained in specific detail in the following paragraphs.

3.1.1. Basic Concepts and Assumptions

The tool has been designed for the simulation of autonomously driven travel segments. Therefore, the driving cycles can be determined for the autonomously driven segments of L2 systems, up to fully autonomous L5 systems. The investigated AV is capable of autonomous driving on well-maintained roadways without human driver intervention. The AV can drive autonomously during the entire cycle.

Foreseeably, AVs will coexist with human-driven vehicles on the road. However, communication between vehicles or between the vehicle and the infrastructure is not yet feasible [44]. This leads to an environment in which the investigated AV can only collect data from its own sensors. Other vehicles on the road are therefore assumed to be driven by humans.

For simplification, only longitudinal dynamics were considered for all existing driving cycles [8], due to their use for evaluating the consumption and emissions of the powertrain.

The lateral dynamics were neglected because their impact on the powertrain concept design is marginal. A purely longitudinal evaluation offers the option of executing the driving cycles on a vehicle test bench. In the cycles generated by the tool, the AV merely drives longitudinally along a virtual, straight road. Although the AV can overtake the front vehicle, the lateral dynamics and steering are disregarded.

The longitudinal movement of the AV is controlled with an ACC system. In addition, the AV can decide whether to overtake the front vehicle. The driving style of the AV affects the parameters in the ACC controller and the overtaking logic.

In this paper, we consider only autonomous passenger vehicles, so the respective user requirements and the driving style were studied, including driving dynamics, driving behavior, and driving conditions. Nevertheless, this methodology can be used for commercial vehicles with appropriate modifications.

3.1.2. Structure of the Tool

The structure of the tool was developed on the basis of these assumptions (Figure 2). The driving style of the AV is the input of the tool, and the driving cycle is the output. In addition, driving conditions such as traffic density, road category, and speed limits can be entered into the tool as settings.
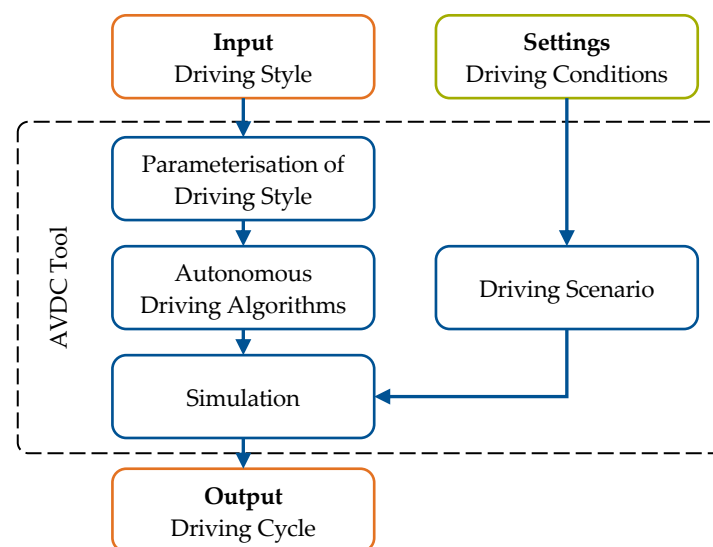

Figure 2. Structure of the AVDC Tool.

The driving style input is converted into the parameters of the driving algorithms, consisting of the ACC system and the overtaking decision. In parallel, the driving scenario is generated based on the driving conditions. The AV simulates driving in the generated scenario to record the driving cycle. The tool was implemented via MATLAB/Simulink.

According to this structure, the three main tool components were the driving style, the driving algorithm, and the driving scenario.

3.2. Criterion for Driving Style

The driving style of an AV impacts the passengers' evaluation of the ride within the vehicle, and thus the vehicle concept itself. Furthermore, different passengers prefer different driving styles in different settings. Therefore, in order to focus on the passenger perspective, customer-relevant properties—a metric commonly used in the automotive sector—were applied to evaluate driving style aspects on a nominal scale from 5 to 10 [45]. We defined the driving styles with the four aspects: comfort, safety, swiftness, and economy.

3.2.1. Comfort

The first step in criteria development was that of choosing appropriate indicators. In the literature, acceleration a and jerk j are commonly used as indicators for ride comfort [34,46–48].

The human body has different levels of sensitivity at different vibration frequencies. ISO 2631-1 systematically studied the effects of mechanical vibration on humans [49,50]. For seated people, as for passengers in vehicles, there are two frequency weightings, one for comfort (W_d) and one for motion sickness under longitudinal vibration (W_f) (Figure 3). These two aspects have different biological mechanisms and therefore different frequency weightings. The acceleration weighted with W_d and W_f are called a_{comf} and a_{sick}.
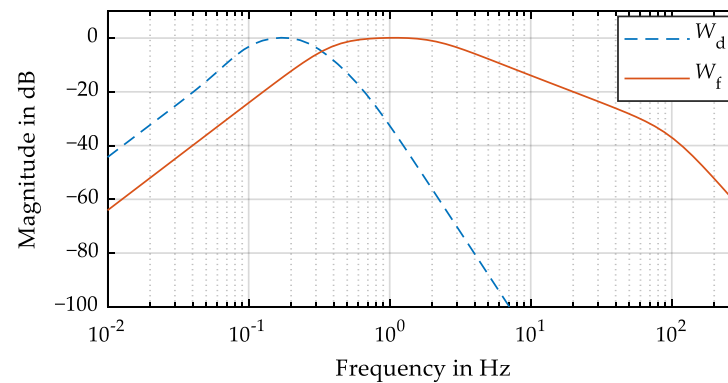

Figure 3. Frequency weighting curves for comfort and motion sickness [49].

The instantaneous values were converted into average values in order to develop the indicators for evaluating an entire trip. We used the root mean square (RMS), which is recommended by ISO 2631-1 [49], where the higher value has a greater influence and should then be given a higher weight. Therefore, three comfort indicators were chosen—$a_{comf,RMS}$, $a_{sick,RMS}$, and j_{RMS}.

These indicators were then scaled into ratings between 5 and 10. For this purpose, we used driving data as reference values. A VW ID.3 and a Tesla Model 3 were driven around Munich for data collection [51]. Both test vehicles were equipped with OBD loggers and smartphones for measurement. The measured signals from two devices were merged into one speed signal with an additional plausibility check. The valid data meeting the following criteria were used for further scaling:

- The driving segment was longer than 1 km.
- The speed signal was continuous and without sudden changes.
- The measured speeds from the OBD and the smartphone varied by a maximum of 5%.

Using these criteria, a total of 393 driving segments with a total distance of 1006 km and duration of 12.6 h were selected. Since the GPS sensor caused strong signal noise, the signal was filtered with a low-pass filter.

The comfort indicators developed were then applied to these driving data. Figure 4 shows the distribution of the three indicators and their fitting of normal distribution, the parameters for which are listed in Table 1.

The indicators were scaled using the distribution function of the normal distribution, value from 0 to 1. Figure 5 shows the distribution function P_{comf} of $a_{comf,RMS}$. The other two indicators were scaled in the same way.

Table 1. Parameters for normal distribution of comfort indicators.

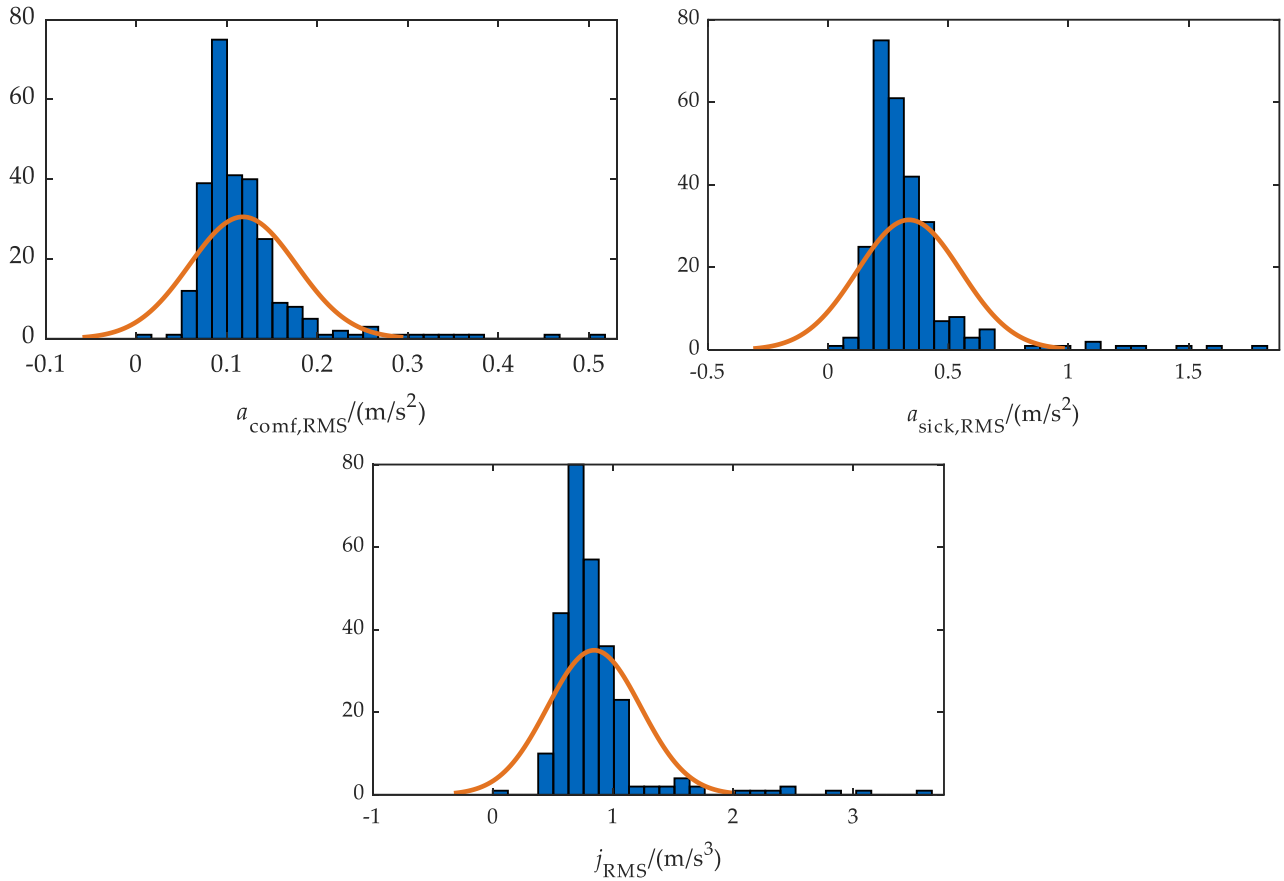| Indicator	Unit	μ	σ
$a_{\text{comf,RMS}}$	m/s^2	0.1177	0.0591
$a_{\text{sick,RMS}}$	m/s^2	0.3365	0.2160
j_{RMS}	m/s^3	0.8438	0.3890

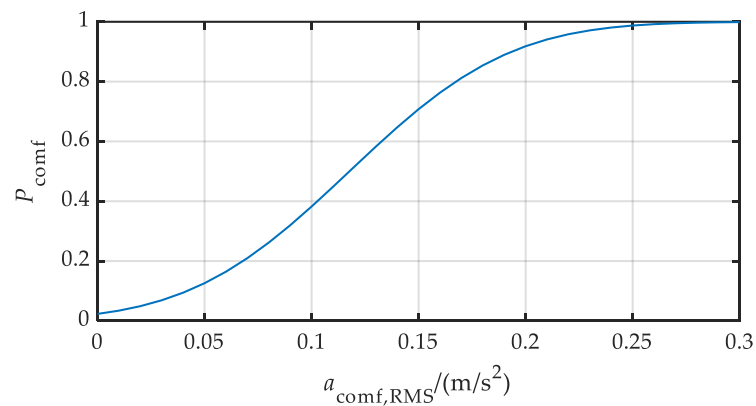**Figure 4.** Distributions of comfort indicators in driving data.

Figure 5. Distribution function of a comfort indicator.

To assess an overall comfort rating, the three scaled indicators P_{comf}, P_{sick}, and P_j need to be merged into a single value. We combined the three values compared to norm of vector

and scaled the minimum and maximum value to rating 4 and 10 to calculate the comfort rating *Comf*:

$$Comf = \left(1 - \frac{\sqrt{P_{\mathrm{comf}}^2 + P_{\mathrm{sick}}^2 + P_j^2}}{\sqrt{3}}\right) \times 6 + 4. \tag{1}$$

Although the minimum input for driving style aspects was 5 in the AVDC Tool, the indicator was scaled with a minimum of 4. Thus, given that it is undesirable, very poor travel comfort could be avoided in the generated cycle.

3.2.2. Safety

As an aspect of driving style, safety refers to passengers' feeling of safety, rather than freedom from accidents, as all AVs should be running accident-free. Subjective safety is a customer-relevant property, as different passengers could have different preferences.

We applied the safety margin *SM* from Lu et al. [37,38], whose definition is given below:

$$SM = 1 - \left(v_{\mathrm{ego}}\, \tau_{\mathrm{rea}} + \frac{v_{\mathrm{ego}}^2}{2a_{\mathrm{B,ego}}} - \frac{v_{\mathrm{front}}^2}{2a_{\mathrm{B,front}}}\right)/d, \tag{2}$$

where v_{ego} and v_{front} are the speed of the ego AV and the front vehicle, d is the distance to the front vehicle, τ_{rea} is the reaction time for braking, and $a_{\mathrm{B,ego}}$ and $a_{\mathrm{B,front}}$ are the braking decelerations of both vehicles.

According to Lu et al., the typical value for τ_{rea} is 0.15 s, and the braking deceleration equals to 0.75 g for used tires on a flat road surface [37]. Finally, this results in the simplified Equation (2):

$$SM = 1 - \left[0.15\mathrm{s}\, v_{\mathrm{ego}} + \frac{(v_{\mathrm{ego}} + v_{\mathrm{front}})(v_{\mathrm{ego}} - v_{\mathrm{front}})}{1.5\,\mathrm{g}}\right]/d. \tag{3}$$

To evaluate the safety of the whole trip, the *SM* calculated with RMS. In contrast to the comfort indicators, a lower *SM* represents a greater hazard where greater weight should be placed. Therefore, only the RMS of the subtrahend was calculated:

$$SM_{\mathrm{RMS}} = 1 - \left\{\left[0.15\mathrm{s}\, v_{\mathrm{ego}} + \frac{(v_{\mathrm{ego}} + v_{\mathrm{front}})(v_{\mathrm{ego}} - v_{\mathrm{front}})}{1.5\,\mathrm{g}}\right]/d\right\}_{\mathrm{RMS}}. \tag{4}$$

Thereafter, this indicator was scaled with the driving data into a rating. In Equation (4), the distance and speed of front vehicle, which are not measured in most data collections, are required. Lu et al. [37] provided the distribution of *SM* values from 34 taxi rides in Beijing (Figure 6).

At several data points, the *SM* was larger than 1 because the subtrahend of Equation (4) was negative. This was achieved when the ego vehicle was at a large distance from the front vehicle and the distance was increasing, which can be considered a no-risk situation. Therefore, these negative values were disregarded (set to zero) when calculating the RMS, leading to an SM_{RMS} smaller than 1. Consequently, only the distribution with $SM < 1$ was used for the scaling. The cumulative distribution $P(SM = 1)$ was given a rating of 10 and $P(SM = -\infty)$ was given a rating of 4.
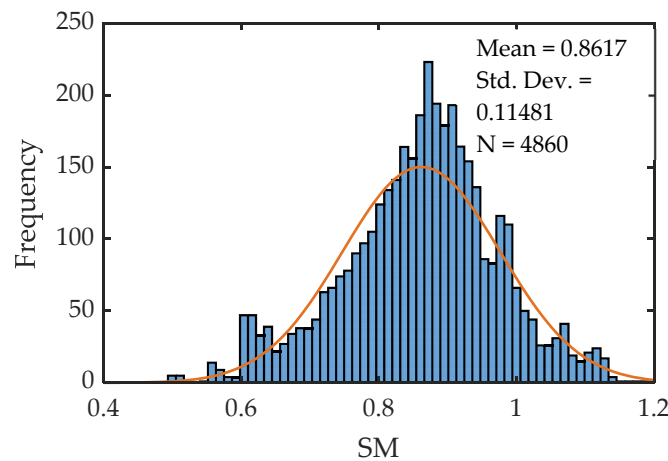
Figure 6. Histogram and distribution of *SM* data [37].

3.2.3. Swiftness

In contrast to comfort and safety, swiftness is an objective aspect whose main criterion for customers is travel time. For certain passengers, the shortest possible time on the road is important. However, the actual travel time is strongly dependent on the distance travelled and the road conditions, whereas driving style has only a limited influence. Therefore, the real travel time t_{trip} was normalized with the minimum travel time t_{min}, which is the time required if the vehicle always drives at the speed limit v_{max} on the entire route s:

$$t_{\text{min}} = \int_0^s \frac{dx}{v_{\text{max}}(x)}, \tag{5}$$

$$t_{\text{norm}} = \frac{t_{\text{trip}}}{t_{\text{min}}} \tag{6}$$

According to German regulations, the speed limit is 50 km/h in the city and 100 km/h on rural roads. There is no legal speed limit on the German motorway, so the recommended speed of 130 km/h was used.

The normalized travel time t_{norm} was no longer dependent on the road categories and distances, but it was still influenced by the driving scenario. Therefore, the scaling was carried out for the value range of the indicator in the simulation. The maximum and minimum possible travel time was calculated within the reasonable range of all control parameters (the parameters and their ranges are defined in Section 3.5.1). According to the simulation results, the upper and lower limits were 2.1 and 1.9, respectively.

The distribution function of the normal distribution was used for scaling the comfort and safety indicators. Hence, the curve of the scaling had an S-shape (e.g., Figure 5). With an S-curve, the function value is degressive at both boundaries. The S-shaped scaling is suitable for subjective customer values, since the characteristics of various vehicle models and the expectations of different customers are similar to the normal distribution [52]. However, the objective variables, such as travel time and consumption, are different. When travel time or consumption is reduced, further reduction will be more difficult and costly. Therefore, the value should not be degressive.

For this reason, we propose scaling the objective indicators logarithmically, whereby an equal percentage improvement value leads to the same difference in rating. Figure 7 shows the logarithmic (7) and linear scaling (8) of the t_{norm}.

$$y_{log}(x) = b\,ln(a\,x), \tag{7}$$

$$y_{lin}(x) = a\,x + b. \tag{8}$$

The limits for customer values were mapped to ratings of 10 and 5, with which the two coefficients *a* and *b* can be determined. The swiftness rating *Fast* was calculated with the scaling function. Within the range used, the linear scaling approached the logarithmic scaling because the change was small. Thus, linear scaling was used to simplify calculation.
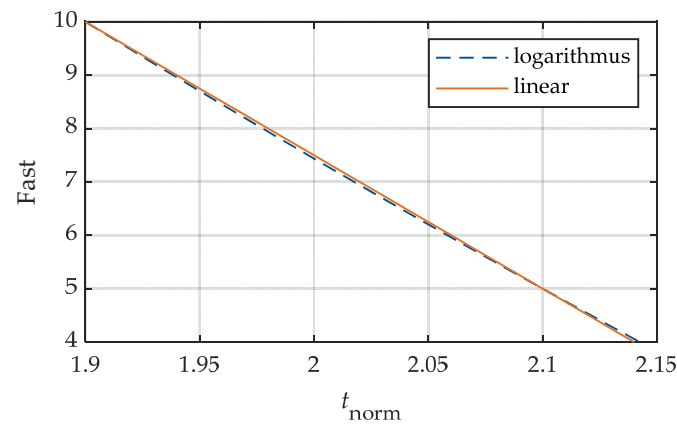

Figure 7. Scaling of the swiftness indicator.

3.2.4. Economy

Whereas swiftness concerns time saving, economy refers to energy saving, which reduces the operating cost of the vehicle. The evaluation of efficiency is one typical application of driving cycles. In this paper, electric driven AVs were investigated, and the consumption is described as the energy consumed per 100 km. In the simulation for the driving cycle, the consumption was calculated using an open-source longitudinal dynamics simulation (LDS) [53]. The simulated speed profile was entered into the LDS, which calculated the electrical energy consumed during the driving cycle according to the vehicle parameters.

To exclude the influence of the route, the consumption of the AV $b_{100\text{km,el}}$ was normalized with a reference consumption $b_{100\text{km,ref}}$ of the front vehicle, which followed a standard cycle. The normalized consumption b_{norm} represents the economy:

$$b_{\text{norm}} = \frac{b_{100\text{km,el}}}{b_{100\text{km,ref}}}. \tag{9}$$

Similar to swiftness, the economy indicator was also scaled linearly with upper and lower limits, which were 20% savings and 20% higher consumption (compared to original standard cycle used for traffic vehicles), respectively. Figure 8 shows the economy indicator scaling.
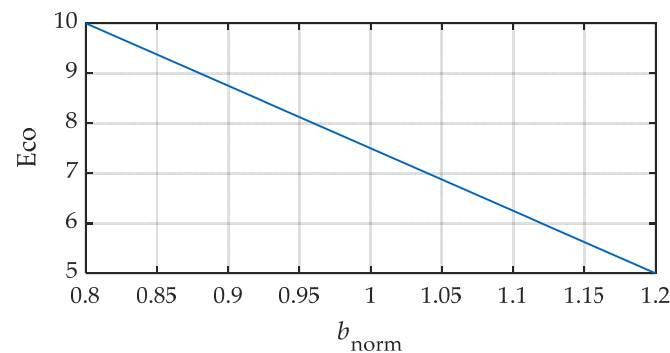

Figure 8. Scaling of the economy indicator.

3.3. Autonomous Driving Algorithms

Given that our focus was on the mixed traffic of AVs and non-AVs during the next decade, known algorithms were chosen for modelling and simulation. According to the concept behind the AVDC Tool, the investigated AV drives along a straight road. Therefore, the AV is controlled by the ACC (Adaptive Cruise Control) system.

The ACC was modelled with a cascade control, consisting of a distance controller and a speed controller [54] (p. 874) (Figure 9). The target distance $x_{\text{rel,set}}$ was equal to the desired time headway t_{set} multiplied by its ego velocity v_{ego}, adding the static distance d_0 to maintain a safe distance at standstill:

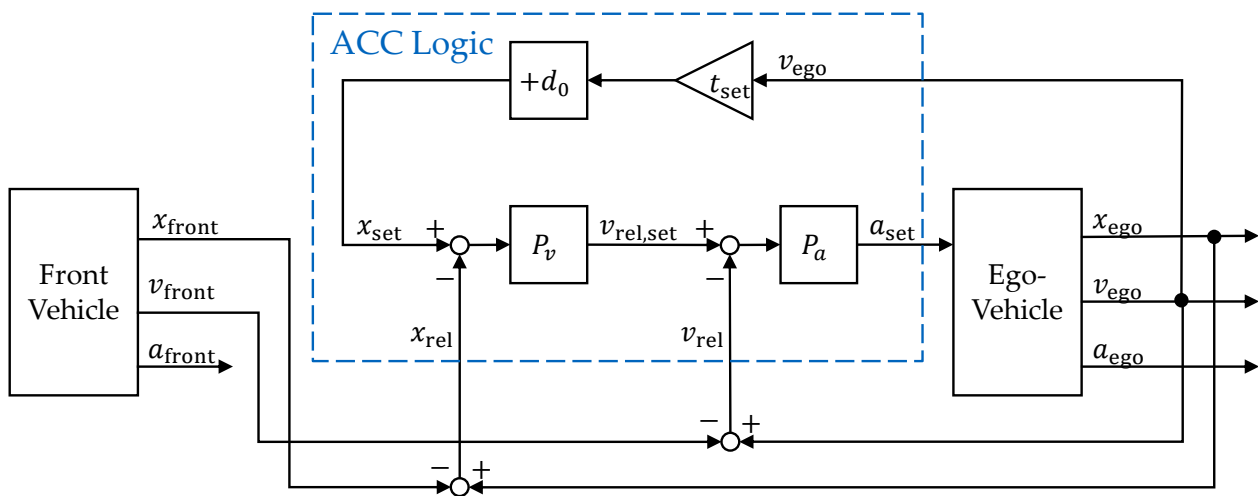$$x_{\text{rel,set}} = v_{\text{ego}}\, t_{\text{set}} + d_0. \tag{10}$$

Figure 9. Block scheme of ACC controller based on [54] (p. 874).

For a simple implementation, the distance and speed controllers were both P-controlled with P-coefficient P_v and P_a. In the tool, the two P-controllers have been modelled as a lookup table, which allows a variable proportional coefficient. For example, different P values could be used for acceleration and deceleration, or for low and high control errors.

When the ego vehicle is not hindered by the front vehicle, the ACC controller operates in free drive mode; the distance controller is not functional, and the speed controller is regulated to the set speed v_{set}.

In order to achieve a comfortable ride using ACC, the output set acceleration a_{set} and its derivation were limited with saturation at the lower and upper limits. ISO 15622:2018 defines the limits of acceleration and jerk of full speed range ACC system [55]. The upper and lower limits are speed-dependent, as shown in Figure 10.

In the standard, only the limit for negative jerk is given [55]. To ensure ride comfort, we defined the upper limit with same absolute value (Figure 11).

In addition to ACC, automatic emergency braking (AEB) was also implemented in the driving algorithms in order to avoid a collision with the front vehicle. When the ACC is set to a comfortable driving style, the AV may not brake with enough deceleration as the front vehicle slows. The AEB can interfere to firmly brake the vehicle and prevent an accident.

During the simulated trip, the ego AV can choose to overtake traffic vehicles. Therefore, overtaking logic is required to decide whether the AV will overtake. Since only 1-D movement in the longitudinal direction was considered by the tool, an overtake was simulated as the masking out of the front vehicle, after which the AV can detect and follow the next vehicle ahead. When the ego AV has been overtaken, the overtaking traffic vehicle cuts in and becomes the new front vehicle for the AV.
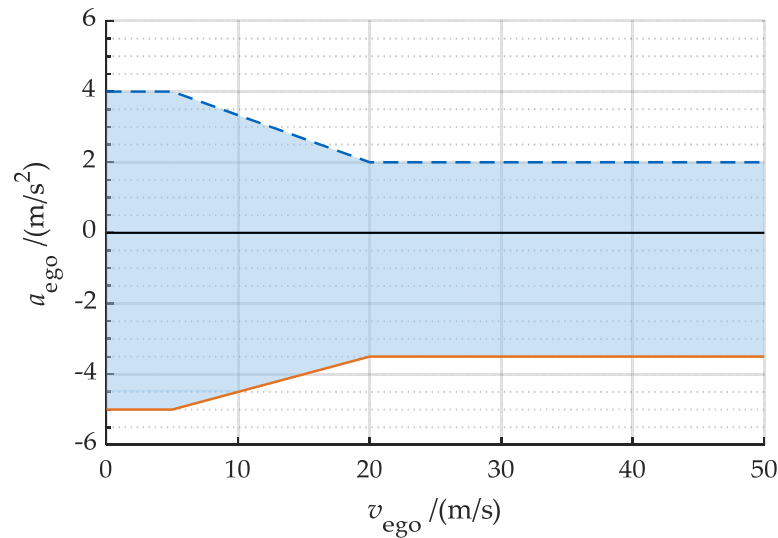
Figure 10. Upper and lower limits of acceleration according to ISO 15622:2018 [55].
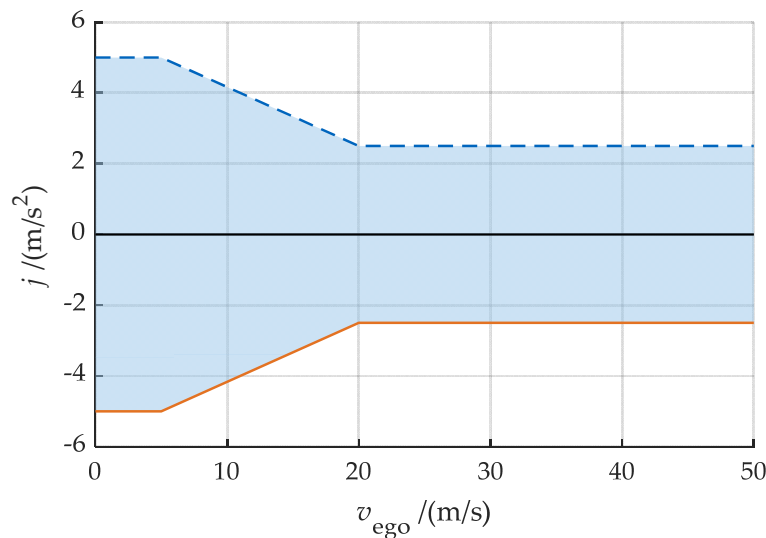
Figure 11. Upper and lower limits of jerk based on [55].

Two criteria were designed for the overtaking logic:

1. The speed of front vehicle v_{front} is lower than the set speed v_{set} by more than the tolerance threshold $v_{\mathrm{ovt,tol}}$:

$$v_{\mathrm{front}} < v_{\mathrm{set}} - v_{\mathrm{ovt,tol}}. \tag{11}$$

2. The estimated distance required for overtake $d_{\mathrm{ovt,req}}$ is shorter than the available distance d_{ovt}, where overtaking is allowed:

$$d_{\mathrm{ovt,req}} < d_{\mathrm{ovt}}. \tag{12}$$

The permission for overtaking and the corresponding d_{ovt} is explained in Section 3.4.

Figure 12 shows the state diagram for the overtaking logic. When all conditions are fulfilled for three seconds, an overtake is initiated by the ego AV. This time delay produces stable overtaking decisions. Otherwise, the state could change rapidly in borderline cases. After the overtaking has been started, the required distance $d_{\mathrm{ovt,req}}$ continues to be examined according to (11). If the available d_{ovt} is no longer sufficient, the overtaking process will be aborted. In this case, no new overtaking attempt can be started for 10 s (to avoid an

attempt-abort loop). When the ego AV is 5 m ahead of the overtaken vehicle, the overtake has been successfully completed.

When the logic is in the overtake state, the set speed of ACC v_{set} is increased by 5% to make the overtake faster and reduce the likelihood of an abort. When the overtake has been completed or aborted, the v_{set} is reset to the normal state.
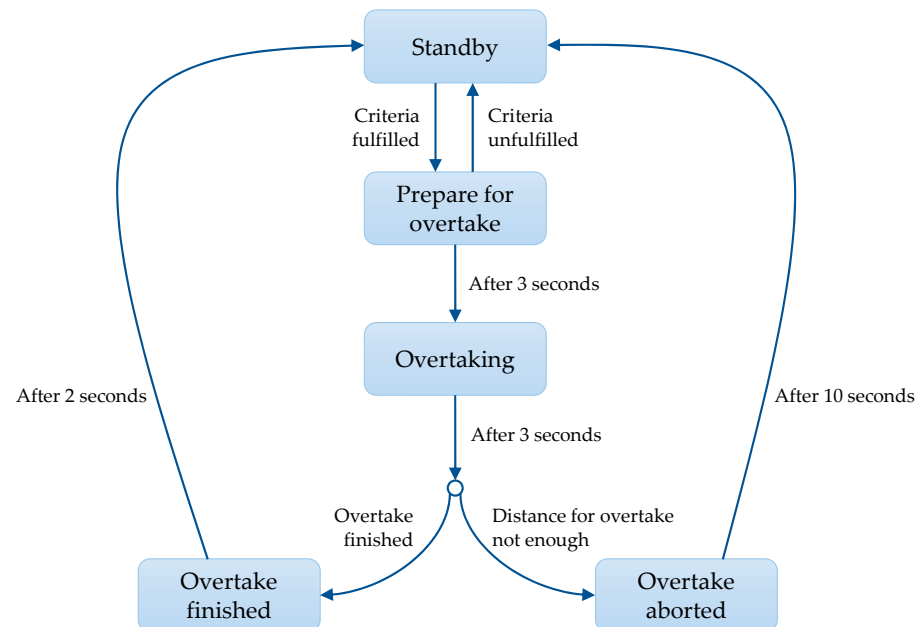

Figure 12. Overtaking logic state diagram.

In addition to algorithms, the sensors and actuators of the AV were also modelled. The modelled AV could use radar and camaras for the implemented ACC functions, which is the industry standard. The sensors were modelled at a 250 m detection rate and can measure the distance and speed of the front vehicle. The latency of measurement was set to 0.2 s, and the measurement error has been neglected in the tool.

The AV being investigated is assumed to have an electrical powertrain. The desired acceleration a_{set} is first limited between 5 m/s^2 and -8 m/s^2, considering the torque of driving motor and the friction of the tires. The powertrain is then modelled as a first-order inertial element with a 0.5 s time constant, where the desired a_{set} is the input, and the actual acceleration a_{ego} is the output.

3.4. Driving Scenario

According to the basic concepts in Section 3.1.1, the ego AV is traveling in mixed traffic consisting of human-driven vehicles and AVs. Since no communication exists between vehicles, all traffic vehicles can be considered to be human-driven. The existing driving cycles, which were developed with real driving data, are intended to represent typical use of the vehicles. Therefore, we used these driving cycles for the traffic.

For simplification, it was assumed that the traffic vehicles were driving at the same time interval and following a certain driving cycle from the same position. Thus, all traffic vehicles were at the same speed and in the same position, but traveling at different times. During the journey, it is possible that the traffic vehicles would overlap at some times, e.g., during a standstill longer than the interval. This overlap was handled in the traffic module, since only the front vehicle can be detected by the ego vehicle, whereas other traffic vehicles have no influence. Furthermore, the traffic vehicles were not affected by the ego vehicle.

The ego vehicle may overtake traffic on those sections of the route where doing so is permitted. Therefore, the route needs to be processed to determine whether overtaking is allowed.

First, it was necessary to increase the sampling rate of the traffic driving cycle. Since the existing driving cycles are normally driven by drivers or robots on the test bench, the speed profile of the cycles is defined in data points per second (1 Hz). The electronic systems of AV can react within the millisecond range, and one second is too long for use as a simulation time step for the autonomous driving algorithms; the ACC cannot control the AV smoothly, and the AEB does not react in time because it intervenes only a few seconds before an accident. For this reason, the simulation time step must be shorter. In the tool, the time step was set to 0.02 s, or 50 Hz. Therefore, the profile was also interpolated to a 50 Hz sampling rate. The modified-Akima interpolation in MATLAB was utilized to prevent overshoots.

Permission for overtaking is determined using the interpolated speed profile. The route sections are marked as permissible for overtaking if they fulfill the following two criteria:

1. The speed is within a window of 15 km/h for at least 20 s. This means that the vehicle travels at an approximately constant speed in the route section. If the speed changes rapidly, overtaking is inappropriate.
2. The minimum speed in the window is higher than 30 km/h. The vehicle drives slowly when hindered by the driving environment, e.g., traffic lights or congestion. In these situations, overtaking is also inappropriate.

Using these criteria, all positions along the route are assessed as to whether an overtake is permissible. The distance available for overtaking d_{ovt} at each position is then calculated. This means the distance to the next point from which overtaking is not allowed. An overtaking operation must be completed within d_{ovt}.

In addition, the ego vehicle can be overtaken by traffic. The vehicles behind the ego vehicle are masked out until they are 20 m ahead of the ego vehicle, i.e., the overtaking traffic vehicle cuts in 20 m in front of the ego vehicle and then becomes detectable. At stops, the ego vehicle stops a few meters (static distance d_0) behind the front vehicle. The rear traffic vehicle drives in front of the ego vehicle and stops at the same position as the front vehicle. The distance does not reach 20 m and the vehicle remains hidden. When the front vehicle starts moving, the ego vehicle can move and follow the same front vehicle.

Furthermore, the road categories need to be identified to determine the speed limit. Under Germany's traffic regulations, the maximum speed limit is 50 km/h in the city and 100 km/h on rural roads. There is no speed limit on German motorways, so the recommended speed of 130 km/h is applied. The road categories are identified for microtrips, which are defined as the sections between two adjacent stops. The road categories are determined according to the highest speed of the microtrip $v_{\text{trip,max}}$ (Table 2). This method is particularly suitable for the driving cycles built with several microtrips selected from different categories, e.g., WLTC [13].

Table 2. Classification of road categories according to the highest speed.

Road Category	Highest Speed in km/h
Urban	$v_{\text{trip,max}} \leq 60$
Rural	$60 < v_{\text{trip,max}} < 110$
Motorway	$v_{\text{trip,max}} \geq 110$

Some driving cycles are designed for a specific road category. Specifically, the European ARTEMIS project has three cycles each for urban roads, rural roads, and motorways [56,57]. In this case, the corresponding category is set for the cycle.

3.5. Parameterization of Driving Style

After the completion of the described modules, it was possible to determine the parameters for different driving styles. As discussed in Section 3.2, four aspects were

defined—comfort, safety, swiftness, and economy. Each aspect was assigned a rating from 5 to 10, where 5 is the lowest but still acceptable, and 10 is best value for users.

Every controller parameter of the AV influences multiple aspects simultaneously. We used data-based modelling to analyze the interdependencies between the aspects and the parameters.

Figure 13 shows the workflow of this process. First, the setting parameters were chosen and used to generate test points with DoE (Design of Experiment) (①). The set of test points were then input into simulation and the generated cycles evaluated for driving style aspects (②). These data were used to build the numerical model for each aspect (③). The parameters for different driving styles were generated with these models (④).
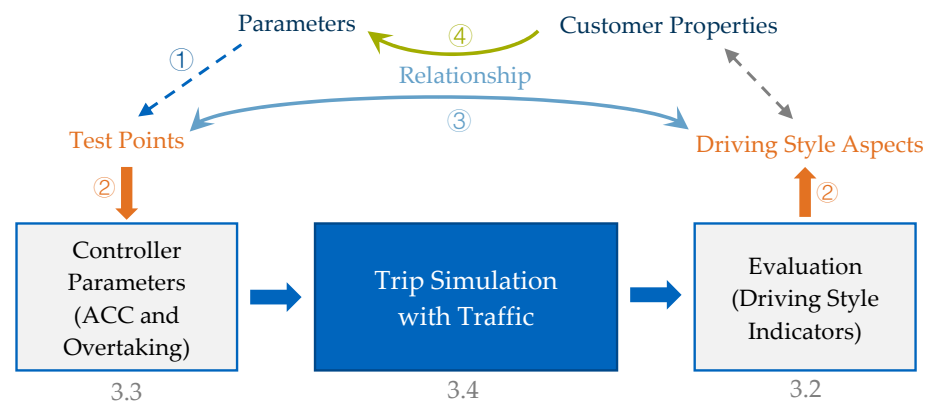

Figure 13. Workflow for parameterizing the driving style.

3.5.1. Definition of Setting Parameters

As setting parameters, we chose eight parameters having a significant influence from among the autonomous driving algorithms (Table 3).

Table 3. AV setting parameters.

Parameter	Unit	Min. Value	Ref. Value	Max. Value	Description
t_{set}	s	0.5	2	3	Set time headways of ACC
P_a	-	0.3	0.7	2	P-coefficient of speed controller
C_{brk}	-	0.66	1	1.5	Coefficient for deceleration
P_v	-	0.03	0.07	0.2	P-coefficient of distance controller
C_{vset}	-	0.8	1	1.2	Coefficient for set speed
a_{max}	m/s^2	1	2	4	Maximum acceleration of ACC
j_{max}	m/s^3	2	5	10	Maximum jerk of ACC
$v_{ovt,tol}$	km/h	5	20	40	Tolerance speed for overtaking

The first seven parameters belong to the ACC system. The t_{set}, P_a, and P_v are explained in Section 3.3. The reference values were determined according to [54]. The coefficient K_{brk} describes the ratio of $P_{a,neg}$ and $P_{v,neg}$ in a negative direction to P_a and P_v in the positive direction:

$$P_{a,neg} = C_{brk} \, P_a, \tag{13}$$

$$P_{v,neg} = C_{brk} \, P_v. \tag{14}$$

Figure 14 shows the speed controller with different P_a in the positive and negative directions.

The coefficient v_{para} represents the relative target speed. The ACC target speed v_{set} is equal to v_{para} times speed limit v_{max}:

$$v_{set} = C_{vset} \, v_{max}. \tag{15}$$

The maximum value of v_{para} is 1.2. When v_{para} is greater than 1, the v_{set} will not exceed the speed limit v_{max} in the city or on rural roads, but the AV can drive faster than the recommend speed of 130 km/h on the highway. Figure 15 shows the v_{set} for different road categories with different C_{vset}.

The limits of acceleration and jerk in the ACC are not fixed values, but rather speed-dependent characteristic curves (Figures 10 and 11). When the limits a_{max} and j_{max} are varied, the shape of the characteristic curve is maintained, i.e., a_{max} and j_{max} are halved at a speed of 20 m/s.
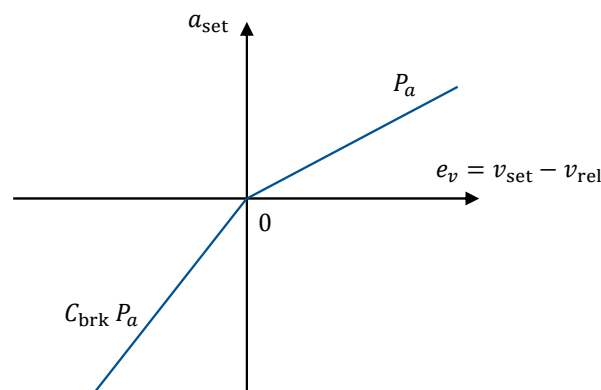

Figure 14. Different P-coefficient in the positive and negative directions.
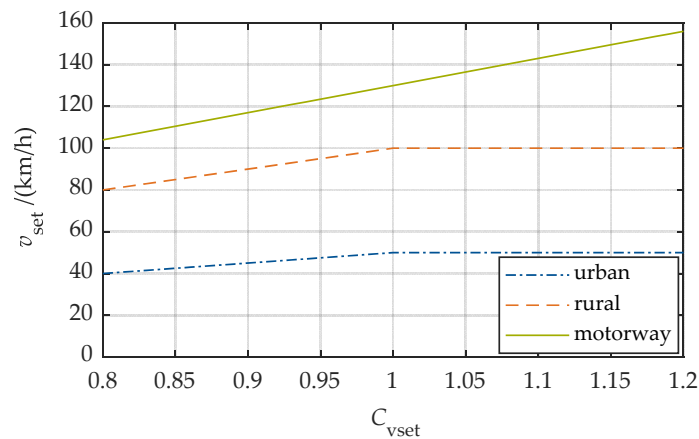

Figure 15. Target speed for different road categories.

The variable $v_{ovt,tol}$ is a parameter in the overtaking logic (10). The higher the $v_{ovt,tol}$, the slower the front vehicle speed that the AV can tolerate.

3.5.2. Design of the Experiment

The setting parameters and their value ranges were entered into the Model Based Calibration toolbox (MBC) of MATLAB [58]. The test points were generated using MBC, with every test point consisting of eight valid values for each parameter. The test points were designed according to the experimental design to fill evenly and completely the high-dimensional space of the input parameters. The Sobol sequence in the MBC toolbox was used for the test design. To determine the appropriate size of the test set, four sets with different sizes were generated: 256, 512, 1024, and 2048 test points. Apart from the test sets,

a validation set was generated using a different method—Latin hypercube—because the test points were generated partially randomly. Therefore, the validation set did not overlap with the test sets. The validation set consisted of 100 test points.

The four test sets and the validation set were input into the simulation. Since we were investigating the traffic environment in Germany, the European ARTEMIS cycles were used for traffic [57]. The WLTC has a significantly lower acceleration than ARTEMIS, so it cannot match the use case in Germany. The three cycles in ARTEMIS—urban road, rural road, and motorway—were simulated consecutively. The driving style indicators for the three road categories were combined for the evaluation of the driving style aspects. Subsequently, each test point was assigned ratings for comfort, safety, swiftness, and economy.

The validation set was filtered according to the results of the simulation, i.e., only the points with a sum of the four aspects exceeding 28 were selected ($Comf + Safe + Fast + Eco > 28$). Points with a lower rating are not included because a poor overall rating means an unfavorable combination of parameters. Out of 100 points in the validation set, 90 points fulfilled this criterion.

3.5.3. Modelling of Driving Style Aspects

Using the data of test sets, models of the four driving style aspects were built individually. The MBC toolbox offers several types of models, among which the Radial-Basis-Function (RBF), Hybrid-RBF, and Gaussian-Process-Model (GPM) methods were used. For each model, numerous model variants were generated using these three methods and were checked with the validation set. The model variant with the smallest root mean square error (RMSE) during the validation was selected. The response models of the four aspects and eight parameters are shown in Appendix A. To determine the appropriate size of the test set, the four test sets were each modelled and validated. The validation RMSEs of the four aspects in four test sets are listed in Table 4.

Table 4. Validation RMSE of the driving style aspects in the test sets.

Valid. RMSE	Comfort	Safety	Swiftness	Economy
256 points	0.506	0.185	0.234	0.079
512 points	0.424	0.157	0.191	0.082
1024 points	0.363	0.141	0.157	0.075
2048 points	0.354	0.123	0.141	0.068

With the increase of the test set, RMSE can be reduced regressively, and no overfitting appears. In the following steps, the test set with 1024 points was used since 2048 points offered only a small advantage and increased the calculation time considerably.

3.5.4. Generation of the Parameter Set

The parameter set consists of the lookup table of the setting parameters. For each desired combination of driving style aspects, the parameter set gives the corresponding values of the eight parameters. The aspects are given as integers between 5 and 10, i.e., each aspect has six possible input values.

The four aspects are coupled with complicated interdependencies. Three of them—comfort, safety, and swiftness—are selected as free inputs, while the fourth—economy—is optimized using the model. For calculation of the parameters, the three free aspects are entered as constraints and the economy is maximized. This optimization problem can then be mathematically represented:

$$\begin{aligned} \max \quad & Eco(t_{\text{set}}, P_a, \ldots, v_{\text{ovt,tol}}) \\ \text{s.t.} \quad & Comf(t_{\text{set}}, P_a, \ldots, v_{\text{ovt,tol}}) = Comf_{\text{set}}, \\ & Safe(t_{\text{set}}, P_a, \ldots, v_{\text{ovt,tol}}) = Safe_{\text{set}}, \\ & Fast(t_{\text{set}}, P_a, \ldots, v_{\text{ovt,tol}}) = Fast_{\text{set}}. \end{aligned} \tag{16}$$

This approach offers several advantages: First, one of the aspects (economy) is optimized. Second, the problem has only three constraints instead of four, so it is easier to find the parameters that satisfy the constraints. Third, the solution to an optimization problem is usually unique. Otherwise, it might be difficult to choose the parameters from among multiple solutions. Economy was chosen as the optimization objective because most customers prefer lower consumption, and thus low operating costs. Reducing consumption is also central to the sustainable development of the automotive industry.

Given that the indicators of comfort and safety were scaled degressively, the rating 10 represents an infinite value for the indicators. Thus, customer ratings of 10 in the constraints are slightly reduced until a solution is available.

Since the three free aspects each have six possible values, the number of combinations of the inputs is $6^3 = 216$. However, not all combinations can be solved through optimization, i.e., some combinations cannot be achieved regardless of the parameters. The achievable range is approximately an inclined plane, which means that three aspects cannot all have high (or low) ratings at the same time. The optimization successfully solves 55 out of 216 combinations. The parameters of 55 combinations constitute the parameter set for the driving style.

The 55 points in the parameter set were again entered into the simulation to validate the modelled driving style ratings. The RMSEs of the model and the simulation are shown in Table 5. The RMSEs of the parameter set somewhat higher than those of the model, but are acceptable.

Table 5. Validation RMSE of the parameter set.

	Comfort	**Safety**	**Swiftness**
Model RMSE	0.363	0.141	0.157
Parameter set RMSE	0.440	0.239	0.255

All work packages for the tool have been developed at this point.

4. Results

A graphical user interface was designed using App Designer in MATLAB, to make it easier for users to interact with the tool. The interface is shown in Appendix B.

The main feature of the AVDC Tool is the generation of driving cycles for different driving styles. 55 styles were configured during the parameterization. In this section, three typical configurations have been selected for presentation and discussion of results:

- Comfortable driving style with $Comf = 10$, $Safe = 9$, $Fast = 6$,
- Safe driving style with $Comf = 8$, $Safe = 10$, $Fast = 5$,
- Swift driving style with $Comf = 7$, $Safe = 6$, $Fast = 10$.

Each driving style selected has a maximum rating of 10 on one of the driving style aspects, so the features of the different aspects are distinct. The parameters of the three driving styles are listed in Table 6, along with a comparison to the reference values.

The three driving styles show clear differences in the parameters. The comfortable driving style has the lowest P_a so the AV reacts smoothly to speed differences. The low v_{para} and high $v_{ovt,tol}$ make the comfortable driving style patient and slow. The safe driving style has some similarities to the comfortable style, e.g., similar t_{set}, low v_{para} and a_{max}, and high $v_{ovt,tol}$. However, the safe driving style has a much higher P_a in order to allow the AV to adapt quickly to the speed of the front vehicle. One typical feature of the safe driving style is a K_{brk} greater than 1, which means the AV tends to brake hard and accelerate gently. For the swift driving style, a short time headway t_{set} is maintained. With high P_a and P_v, and a K_{brk} smaller than 1, the AV can accelerate aggressively. In this driving style, the limitations a_{max} and j_{max} are also increased. The high v_{para} and low $v_{ovt,tol}$ mean that the AV tends to drive fast and will not tolerate a slow front vehicle.

Table 6. Setting parameters for the selected driving styles.

Parameter	Unit	Ref. Value	Comfortable	Safe	Swift
t_{set}	s	2	2.43	2.40	0.65
P_a	-	0.7	0.50	1.43	1.49
C_{brk}	-	1	1.00	1.30	0.86
P_v	-	0.07	0.15	0.04	0.12
C_{vset}	-	1	0.80	0.80	1.06
a_{max}	m/s^2	2	1.93	1.46	3.91
j_{max}	m/s^3	5	5.96	4.52	8.61
$v_{\text{ovt,tol}}$	km/h	20	26.00	20.77	11.16

ARTEMIS cycles were used for the driving scenarios, consisting of three cycles for urban roads, rural roads, and motorways. Thus, autonomous cycles were generated separately for three road categories. Figure 16 shows the cycles for the comfortable driving style.
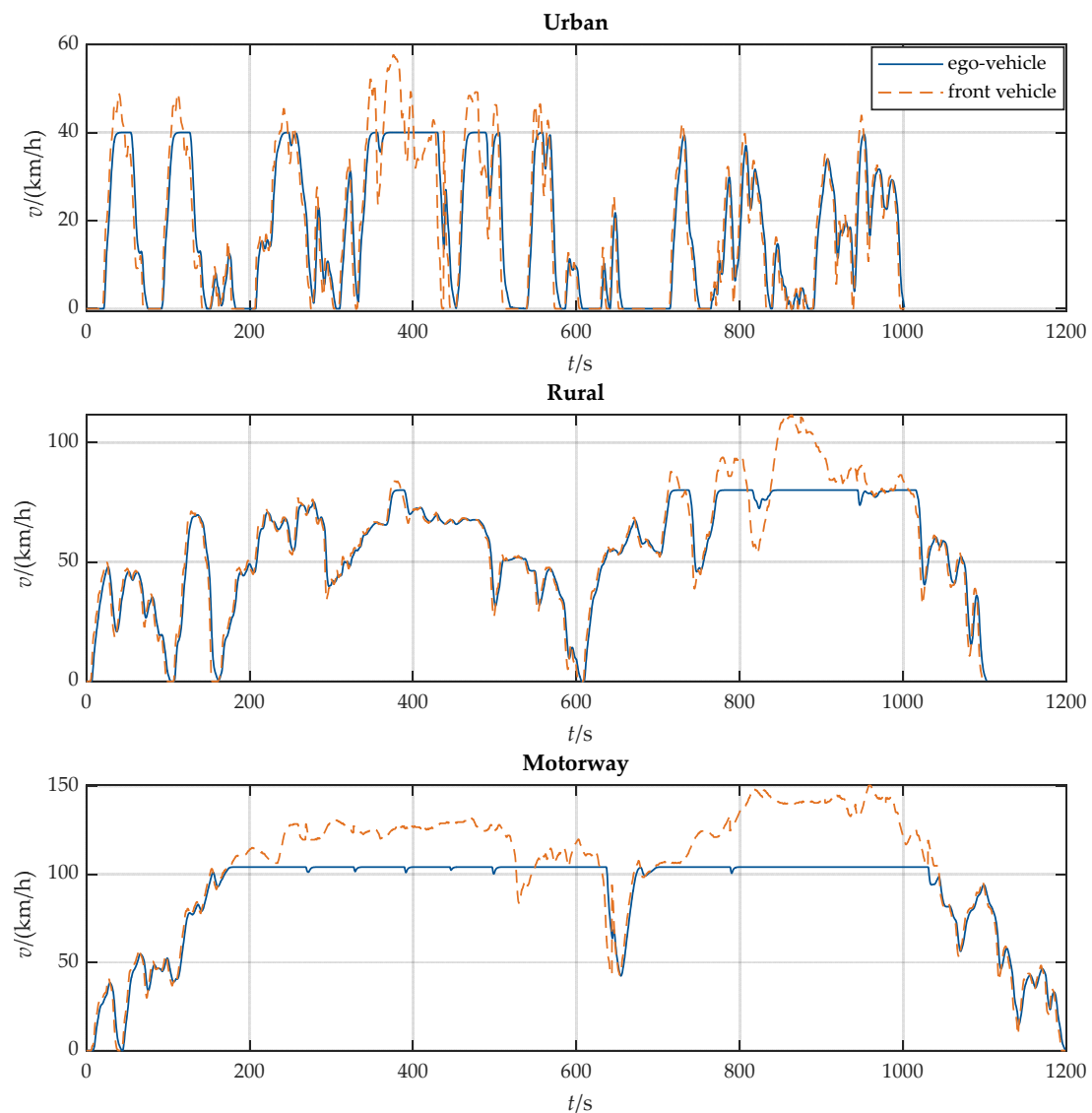
Figure 16. Driving cycles for the comfortable driving style.

With the comfortable driving style, the speed fluctuations of the traffic vehicle are well smoothed to achieve more comfort. Because the AV is driving relatively slow, it was overtaken several times during the cycles on rural road and motorway.

Figure 17 shows the urban cycle of the safe driving style for comparison. Compared to the comfortable style, the speed was adjusted rapidly to match the front vehicle with the safe riding style. The smoothing effect was significantly lower.
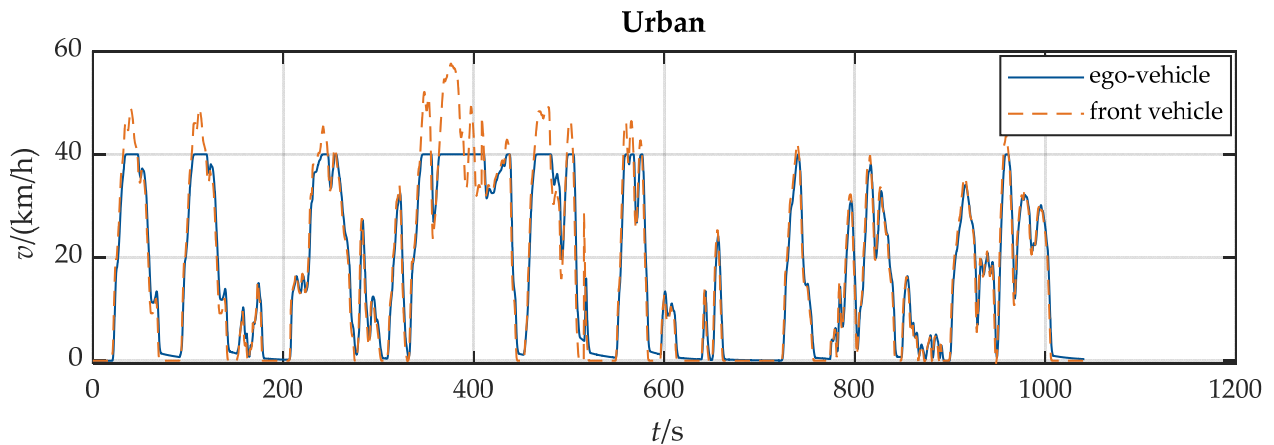
Urban

Figure 17. Urban cycle for the safe driving style.

Figure 18 shows the motorway cycle for the swift driving style. The AV drove at a higher speed and overtook often (marked with green arrows).
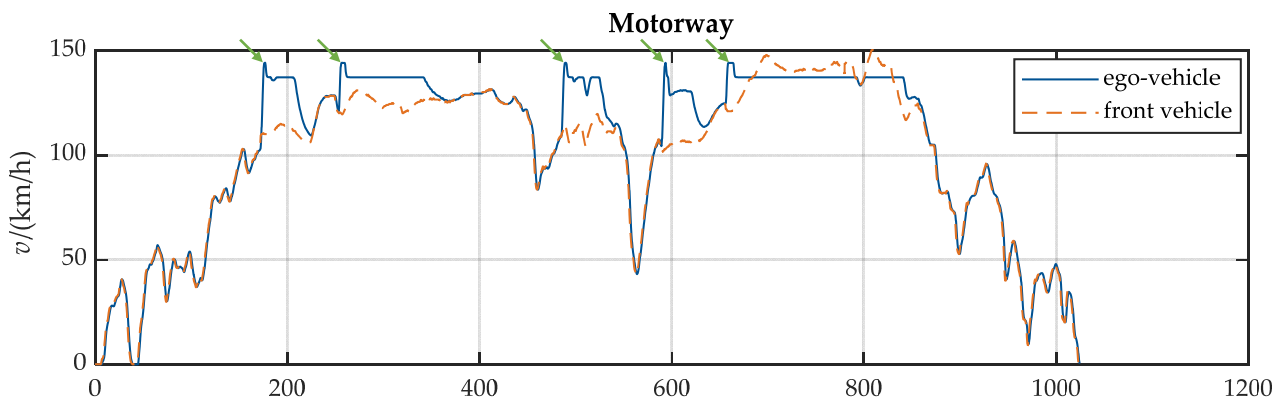
Motorway

Figure 18. Motorway cycle for the swift driving style.

Several attributes of the cycles were calculated and are listed in Table 7 to compare the driving styles comprehensively:

- T—the duration of the driving cycle,
- $\bar{v}$—the average speed during the driving cycle,
- $v_{\text{ego,max}}$—the highest speed during the driving cycle,
- a_{RMS}—the RMS value of acceleration during the driving cycle,
- j_{RMS}—the RMS value of the jerk during the driving cycle,
- $\overline{\frac{1}{TTC}}$—the mean of the reciprocal of TTC during the driving cycle,
- N_{ovt}—the number of vehicles overtaken during the driving cycle (if the ego vehicle is overtaken by traffic, the number is counted as negative).
- $b_{\text{100km,el}}$—the consumption of the drive cycle (in LDS of Tesla Model 3 with rear-wheel drive [53])

As expected, the comfortable driving style had the lowest a_{RMS} and j_{RMS}. The safe driving style had the lowest $\overline{\frac{1}{TTC}}$ and the swift driving style had the shortest T and the highest $\overline{v}$, $v_{ego,max}$ and N_{ovt}. The generated driving cycles were able to demonstrate the characteristics of the different driving styles, thus meeting the objective of the AVDC Tool.

Table 7. Evaluation attributes of the cycles with different driving styles.

Road Category	Driving Style	T s	$\overline{v}$ km/h	$v_{ego,max}$ km/h	a_{RMS} m/s^2	j_{RMS} m/s^3	$\overline{\frac{1}{TTC}}$ 1/s	N_{ovt} -	$b_{100km,el}$ kWh/100 km
urban	original	986	17.8	57.7	0.80	0.95	/	/	14.56
	comfortable	998	17.5	40.0	0.55	0.44	0.038	−1	11.84
	safe	1006	17.3	40.0	0.68	0.78	0.013	−2	12.55
	swift	986	17.8	50.0	0.75	0.86	0.084	0	13.97
rural	original	1076	57.8	111.5	0.64	0.66	/	/	15.61
	comfortable	1099	56.6	80.1	0.47	0.25	0.015	−2	14.42
	safe	1108	56.1	80.1	0.56	0.46	0.006	−3	14.71
	swift	986	63.0	105.0	0.75	1.16	0.053	9	17.20
motorway	original	1063	100.1	150.4	0.56	0.66	/	/	24.44
	comfortable	1195	89.0	104.1	0.39	0.25	0.007	−13	20.13
	safe	1194	89.0	104.1	0.47	0.40	0.003	−13	20.28
	swift	1023	103.9	144.3	0.66	0.63	0.025	4	21.16

5. Discussion

We built the AVDC Tool for AV development, in which context driving style should be considered as one characteristic of an AV, and different customers prefer different driving styles [53,59]. The tool can be used to generate driving cycles that correspond to a specific driving style. When an AV is developed for a specific user group, the AV should run according to the driving style that the group prefers. The corresponding driving cycles could be generated using the tool and used to calculate the energy consumption for the chosen driving style. In addition, the required driving power and force can be calculated during the cycles. This will help the engineers to determine the powertrain specifications. The service life of the components can also be estimated using the generated cycles.

The tool contains three main modules—driving style, driving algorithm, and driving scenario. Well-developed algorithms for automated driving have been implemented in the tool. Driving style has been divided into four aspects—comfort, safety, swiftness, and economy. With reference to previous studies, the indicators for each aspect were selected and then scaled into unified ratings from 5 to 10 using driving data or simulation results. With these evaluation criteria, each journey was evaluated according to the four aspects of driving style. The driving scenario was modelled as a traffic flow on a straight road. The investigated AV drove in the flow and decided for itself which behavior to perform. It could both overtake other vehicles and be overtaken by other vehicles. Such a standardized scenario provided good comparability between different styles.

So far, the tool has been developed in a merely simulative environment, and this methodology has not yet been validated with experiments. The indicators for evaluating driving styles were developed with the help of previous publications. It has not been validated whether the evaluation of comfort and safety correspond to the subjective perception of users. Also, the generated driving cycles have not been tested with real vehicles, so it remains uncertain whether they will meet expectations.

The AV has been modelled with a simple ACC system and overtake logic, which may be outdated when compared to state-of-the-art research on autonomous driving. The

perception of the AV has also been simplified. In further research, the AVDC Tool could be combined with more advanced autonomous driving algorithms.

In this research, we developed the tool for the conditions in Germany. However, the driving conditions are adjustable in the tool, so they can be adapted for other countries or areas as well. The driving scenario defined by the author was simplified and is different to real driving scenarios. In the simulated scenario, the AV drives on a straight road without curves, traffic lights, road junctions, or other elements. Whether these simplifications are appropriate and how much influence they have was not investigated in this context.

As driving cycles for AVs have been little investigated in previous studies, we intend to develop an innovative methodology for doing so. Further research should improve the different modules of the tool in order to achieve more detailed and more accurate results.

6. Conclusions

We have developed the AVDC Tool, which is capable of generating driving cycles for specific AV driving styles. The driving style is defined by way of four aspects—comfort, safety, swiftness, and economy. The first three are input as ratings from 5 to 10 in the tool, while the economy will be optimized. The investigated ego AV drives on a straight road together with traffic vehicles, which run according to the existing driving cycles. The control parameters for the AV are determined by the input driving style. The speed profile of the ego vehicle is recorded as the generated cycle.

This paper focuses on a topic that has been rarely investigated. We have developed a new methodology for generating driving cycles according to AV driving style. Therefore, the main significance of this paper is to propose a methodology for generating AV driving cycles.

Appendix A. Response Models of the Parameters

Appendix B. GUI of the AVDC Tool
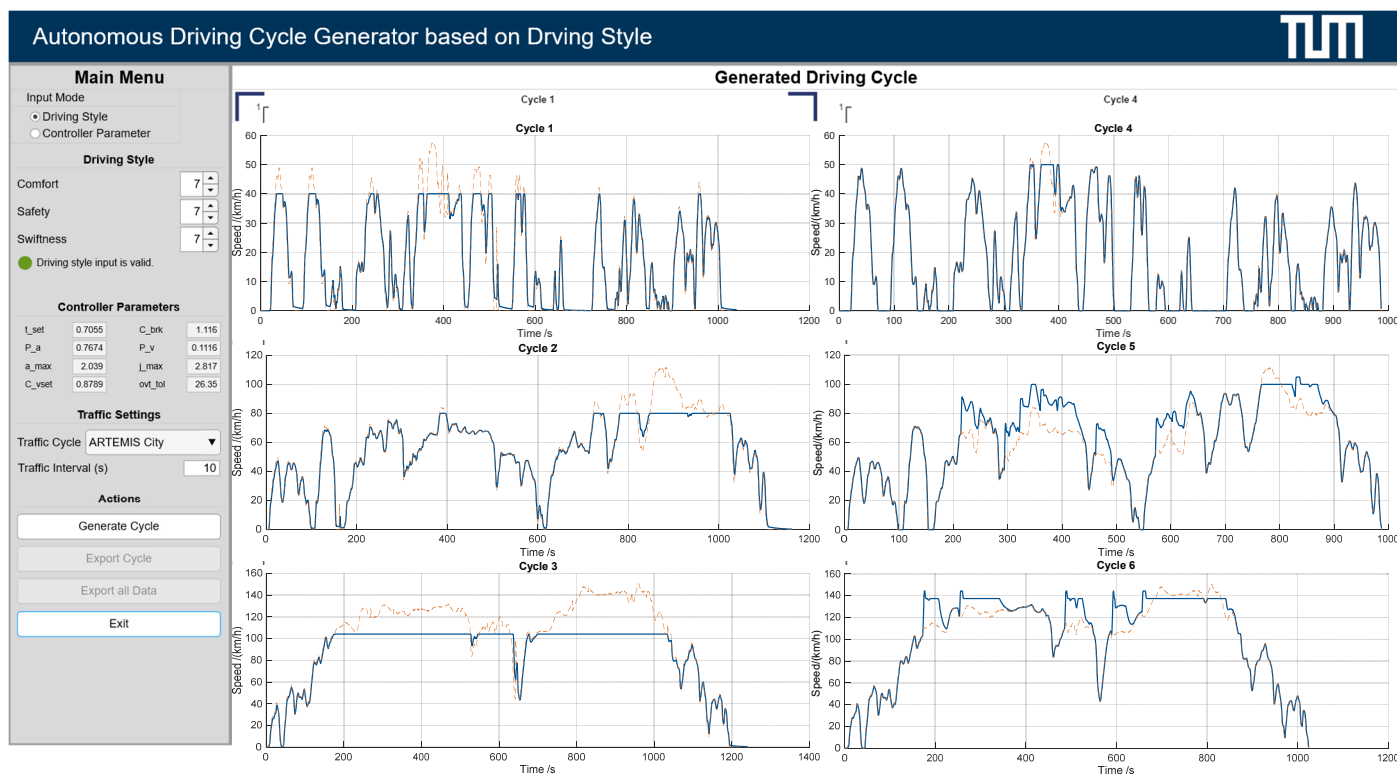
References

1. Yurtsever, E.; Lambert, J.; Carballo, A.; Takeda, K. A Survey of Autonomous Driving: Common Practices and Emerging Technologies. *IEEE Access* **2020**, *8*, 58443–58469. [CrossRef]
2. Mallozzi, P.; Pelliccione, P.; Knauss, A.; Berger, C.; Mohammadiha, N. Autonomous Vehicles: State of the Art, Future Trends, and Challenges. In *Automotive Systems and Software Engineering*; Dajsuren, Y., van den Brand, M., Eds.; Springer: Berlin/Heidelberg, Germany, 2019; pp. 347–367, ISBN 978-3-030-12156-3.
3. Shreyas, V.; Bharadwaj, S.N.; Srinidhi, S.; Ankith, K.U.; Rajendra, A.B. Self-driving Cars: An Overview of Various Autonomous Driving Systems. In *Advances in Data and Information Sciences: Proceedings of ICDIS 2019*; Kolhe, M., Tiwari, S., Trivedi, M.C., Mishra, K.K., Eds.; Springer: Singapore, 2020; pp. 361–371, ISBN 978-981-15-0693-2.
4. Koenig, A.; Schockenhoff, F.; Koch, A.; Lienkamp, M. Concept Design Optimization of Autonomous and Electric Vehicles. In Proceedings of the 2019 8th International Conference on Power Science and Engineering (ICPSE), Dublin, Ireland, 2–4 December 2019; IEEE: New York, NY, USA, 2019; pp. 44–49, ISBN 978-1-7281-6081-8.
5. *Regulation (EU) 2019/631 of the European Parliament and of the Council of 17 April 2019 Setting CO2 Emission Performance Standards for New Passenger Cars and for New Light Commercial Vehicles, and Repealing REGULATIONS (EC) No 443/2009 and (EU) No 510/2011*; Publications Office of the European Union: Luxembourg, 2019.
6. Kim, M.-J.; Peng, H. Power management and design optimization of fuel cell/battery hybrid vehicles. *J. Power Sources* **2007**, *165*, 819–832. [CrossRef]
7. Carraro, E.; Morandin, M.; Bianchi, N. Traction PMASR Motor Optimization According to a Given Driving Cycle. *IEEE Trans. Ind. Appl.* **2016**, *52*, 209–216. [CrossRef]
8. Barlow, T.J.; Latham, S.; McCrae, I.S.; Boulter, P.G. *A Reference Book of Driving Cycles for Use in the Measurement of Road Vehicle Emissions*; Version 3; TRL Limited: Wokingham, UK, 2009.
9. Duan, X.; Schockenhoff, F. Autonomous Vehicle Driving Cycle Tool. Available online: https://github.com/TUMFTM/AV_Driving_Cycles (accessed on 9 April 2022).
10. The MathWorks, Inc. Simulink—Simulation and Model-Based Design. Available online: https://ww2.mathworks.cn/en/products/simulink.html (accessed on 9 April 2022).
11. SAE International. SAE Levels of Driving Automation™ Refined for Clarity and International Audience. Available online: https://www.sae.org/blog/sae-j3016-update (accessed on 14 March 2022).
12. Zhang, X.; Zhao, D.-J.; Shen, J.-M. A Synthesis of Methodologies and Practices for Developing Driving Cycles. *Energy Procedia* **2012**, *16*, 1868–1873. [CrossRef]

13. Tutuianu, M.; Bonnel, P.; Ciuffo, B.; Haniu, T.; Ichikawa, N.; Marotta, A.; Pavlovic, J.; Steven, H. Development of the World-wide harmonized Light duty Test Cycle (WLTC) and a possible pathway for its introduction in the European legislation. *Transp. Res. Part D Transp. Environ.* **2015**, *40*, 61–75. [CrossRef]

14. *GB/T 38146.1-2019*; China Automotive Test Cycle—Part 1: Light-Duty Vehicles. China National Standardization Administration: Beijing, China, 2019.

15. Yang, Z. Factsheet: Japan Light-Duty Vehicle Efficiency Standards. Available online: https://theicct.org/sites/default/files/Japan_PVstds-facts_jan2015.pdf (accessed on 5 December 2021).

16. Tong, H.Y.; Hung, W.T. A Framework for Developing Driving Cycles with On-Road Driving Data. *Transp. Rev.* **2010**, *30*, 589–615. [CrossRef]

17. Galgamuwa, U.; Perera, L.; Bandara, S. Developing a General Methodology for Driving Cycle Construction: Comparison of Various Established Driving Cycles in the World to Propose a General Approach. *J. Transp. Technol.* **2015**, *5*, 191–203. [CrossRef]

18. Zähringer, M.; Kalt, S.; Lienkamp, M. Compressed Driving Cycles Using Markov Chains for Vehicle Powertrain Design. *World Electr. Veh. J.* **2020**, *11*, 52. [CrossRef]

19. Elander, J.; West, R.; French, D. Behavioral correlates of individual differences in road-traffic crash risk: An examination method and findings. *Psychol. Bull.* **1993**, *113*, 279–294. [CrossRef]

20. Sagberg, F.; Selpi; Piccinini, G.F.B.; Engström, J. A Review of Research on Driving Styles and Road Safety. *Hum. Factors* **2015**, *57*, 1248–1275. [CrossRef]

21. Eboli, L.; Mazzulla, G.; Pungillo, G. How drivers' characteristics can affect driving style. *Transp. Res. Procedia* **2017**, *27*, 945–952. [CrossRef]

22. Gurusinghe, G.S.; Nakatsuji, T.; Azuta, Y.; Ranjitkar, P.; Tanaboriboon, Y. Multiple Car-Following Data with Real-Time Kinematic Global Positioning System. *Transp. Res. Rec.* **2002**, *1802*, 166–180. [CrossRef]

23. Sun, P.; Wang, X.; Zhu, M. Modeling Car-Following Behavior on Freeways Considering Driving Style. *J. Transp. Eng. Part A Syst.* **2021**, *147*, 4021083. [CrossRef]

24. van Mierlo, J.; Maggetto, G.; van de Burgwal, E.; Gense, R. Driving style and traffic measures-influence on vehicle emissions and fuel consumption. *Proc. Inst. Mech. Eng. Part D J. Automob. Eng.* **2004**, *218*, 43–50. [CrossRef]

25. Felipe, J.; Amarillo, J.C.; Naranjo, J.E.; Serradilla, F.; Diaz, A. Energy Consumption Estimation in Electric Vehicles Considering Driving Style. In Proceedings of the 2015 IEEE 18th International Conference on Intelligent Transportation Systems—(ITSC 2015), Gran Canaria, Spain, 15–18 September 2015; IEEE: New York, NY, USA, 2015; pp. 101–106, ISBN 978-1-4673-6596-3.

26. Berry, I.M. The Effects of Driving Style and Vehicle Performance on the Real-World Fuel Consumption of U.S. Light-Duty Vehicles. Master's Thesis, Massachusetts Institute of Technology, Cambridge, MA, USA, 2010.

27. Elbanhawi, M.; Simic, M.; Jazar, R. In the Passenger Seat: Investigating Ride Comfort Measures in Autonomous Cars. *IEEE Intell. Transport. Syst. Mag.* **2015**, *7*, 4–17. [CrossRef]

28. Kottenhoff, K. Driving Styles and the Effect on Passengers: Developing Ride Comfort Indicators. 2016. Available online: http://www.diva-portal.org/smash/get/diva2:898005/FULLTEXT01.pdf (accessed on 26 August 2021).

29. Hashimoto, T.; Yanagisawa, H. Risk Feeling Index of Autonomous Vehicle Behavior. In Proceedings of the 6th International Symposium on Affective Science and Engineering (ISASE 2020), Tokyo, Japan, 15–16 March 2020; pp. 1–4. [CrossRef]

30. Qiao, X.; Zheng, L.; Li, Y.; Ren, Y.; Zhang, Z.; Zhang, Z.; Qiu, L. Characterization of the Driving Style by State–Action Semantic Plane Based on the Bayesian Nonparametric Approach. *Appl. Sci.* **2021**, *11*, 7857. [CrossRef]

31. Murphey, Y.L.; Milton, R.; Kiliaris, L. Driver's style classification using jerk analysis. In Proceedings of the 2009 IEEE Workshop on Computational Intelligence in Vehicles and Vehicular Systems (CIVVS 2009), Nashville, TN, USA, 30 March–2 April 2009; IEEE: Piscataway, NJ, USA, 2009; pp. 23–28, ISBN 978-1-4244-2770-3.

32. Dörr, D.; Grabengiesser, D.; Gauterin, F. Online driving style recognition using fuzzy logic. In Proceedings of the 17th International IEEE Conference on Intelligent Transportation Systems (ITSC), Qingdao, China, 10 August–10 November 2014; IEEE: New York, NY, USA, 2014; pp. 1021–1026, ISBN 978-1-4799-6078-1.

33. Karjanto, J.; Yusof, N.M.; Terken, J.; Delbressine, F.; Hassan, M.Z.; Rauterberg, M. Simulating autonomous driving styles: Accelerations for three road profiles. *MATEC Web Conf.* **2017**, *90*, 1005. [CrossRef]

34. Schockenhoff, F.; Nehse, H.; Lienkamp, M. Maneuver-Based Objectification of User Comfort Affecting Aspects of Driving Style of Autonomous Vehicle Concepts. *Appl. Sci.* **2020**, *10*, 3946. [CrossRef]

35. Jachimczyk, B.; Dziak, D.; Czapla, J.; Damps, P.; Kulesza, W.J. IoT On-Board System for Driving Style Assessment. *Sensors* **2018**, *18*, 1233. [CrossRef]

36. Kondoh, T.; Yamamura, T.; Kitazaki, S.; Kuge, N.; Boer, E.R. Identification of Visual Cues and Quantification of Drivers' Perception of Proximity Risk to the Lead Vehicle in Car-Following Situations. *JMTL* **2008**, *1*, 170–180. [CrossRef]

37. Lu, G.; Cheng, B.; Lin, Q.; Wang, Y. Quantitative indicator of homeostatic risk perception in car following. *Saf. Sci.* **2012**, *50*, 1898–1905. [CrossRef]

38. Zhang, X.; Lu, G.; Cheng, B. Parameters Calibration for Car-Following Model Based Desired Safety Margin. In Proceedings of the International Conference on Optoelectronics and Image Processing (ICOIP), Haiko, China, 11 November–11 December 2010; IEEE: New York, NY, USA, 2010; pp. 97–100, ISBN 978-1-4244-8683-0.

39. Griesche, S.; Nicolay, E.; Assmann, D.; Dotzauer, M.; Käthner, D. Should my car drive as I do? What kind of driving style do drivers prefer for the design of automated driving functions? In Proceedings of the 17 Braunschweiger Symposium AAET, Braunschweig, Germany, 9–11 February 2016.

40. Scherer, S.; Dettmann, A.; Hartwich, F.; Pech, T.; Bullinger, A.C.; Wanielik, G. How the driver wants to be driven—Modelling driving styles in highly automated driving. In Proceedings of the 7. Tagung Fahrerassistenz, Munich, Germany, 25–26 November 2015.

41. Xue, Q.; Wang, K.; Lu, J.J.; Liu, Y. Rapid Driving Style Recognition in Car-Following Using Machine Learning and Vehicle Trajectory Data. *J. Adv. Transp.* **2019**, *2019*, 9085238. [CrossRef]

42. Mersky, A.C.; Samaras, C. Fuel economy testing of autonomous vehicles. *Transp. Res. Part C Emerg. Technol.* **2016**, *65*, 31–48. [CrossRef]

43. Roshdi, M.; Nayeer, N.; Elmahgiubi, M.; Agrawal, A.; Garcia, D.E. A Unified Evaluation Framework for Autonomous Driving Vehicles. In Proceedings of the 2020 IEEE Intelligent Vehicles Symposium (IV), Las Vegas, NV, USA, 19 October–13 November 2020; IEEE: New York, NY, USA, 2020; pp. 1277–1282, ISBN 978-1-7281-6673-5.

44. Costandoiu, A.; Leba, M. Convergence of V2X communication systems and next generation networks. *IOP Conf. Ser. Mater. Sci. Eng.* **2019**, *477*, 12052. [CrossRef]

45. Schockenhoff, F.; König, A.; Koch, A.; Lienkamp, M. Customer-Relevant Properties of Autonomous Vehicle Concepts. *Procedia CIRP* **2020**, *91*, 55–60. [CrossRef]

46. Bae, I.; Moon, J.; Seo, J. Toward a Comfortable Driving Experience for a Self-Driving Shuttle Bus. *Electronics* **2019**, *8*, 943. [CrossRef]

47. Bellem, H. Comfort in Automated Driving: Analysis of Driving Style Preference in Automated Driving. Ph.D. Thesis, Technischen Universität Chemnitz, Chemnitz, Germany, 2018.

48. Bellem, H.; Schönenberg, T.; Krems, J.F.; Schrauf, M. Objective metrics of comfort: Developing a driving style for highly automated vehicles. *Transp. Res. Part F Traffic Psychol. Behav.* **2016**, *41*, 45–54. [CrossRef]

49. *13.160 (ISO 2631-1:1997)*; Mechanical Vibration and Shock—Evaluation of Human Exposure to Whole-Body Vibration—Part 1: General Requirements. International Organization for Standardization: Geneva, Switzerland, 1997.

50. *13.160 (ISO 2631-1:1997/AMD 1:2010)*; Mechanical Vibration and Shock—Evaluation of Human Exposure to Whole-Body Vibration—Part 1: General Requirements—Amendment 1. International Organization for Standardization: Geneva, Switzerland, 2010.

51. Wassiliadis, N.; Steinsträter, M.; Schreiber, M.; Rosner, P.; Nicoletti, L.; Schmid, F.; Ank, M.; Teichert, O.; Wildfeuer, L.; Schneider, J.; et al. Quantifying the state of the art of electric powertrains in battery electric vehicles: Range, efficiency, and lifetime from component to system level of the Volkswagen ID.3. *eTransportation* **2022**, *12*, 100167. [CrossRef]

52. Langer, L. *Ableitung Konzeptbestimmender Technischer Werte Autonomer Fahrzeuge anhand Einer Marktanalyse*; Semesterarbeit; Lehrstuhl für Fahrzeugtechnik: Munich, Germany, 2021.

53. König, A.; Nicoletti, L.; Kalt, S.; Müller, K.; Koch, A.; Lienkamp, M. An Open-Source Modular Quasi-Static Longitudinal Simulation for Full Electric Vehicles. In Proceedings of the 2020 Fifteenth International Conference on Ecological Vehicles and Renewable Energies (EVER), Monte-Carlo, Monaco, 10–12 September 2020; IEEE: New York, NY, USA, 2020; pp. 1–9, ISBN 978-1-7281-5641-5.

54. Winner, H.; Hakuli, S.; Lotz, F.; Singer, C. *Handbuch Fahrerassistenzsysteme: Grundlagen, Komponenten und Systeme für Aktive Sicherheit und Komfort*; 3. Auflage; Springer Vieweg: Wiesbaden, Germany, 2015; ISBN 978-3-658-05734-3.

55. *03.220.20 (ISO 15622:2018)*; Intelligent Transport Systems—Adaptive Cruise Control Systems—Performance Requirements and Test Procedures. International Organization for Standardization: Geneva, Switzerland, 2018.

56. André, M.; Keller, M.; Sjödin, Å.; Gadrat, M.; Crae, I.M.; Dilara, P. The ARTEMIS European Tools for Estimating the Transport Pollutant Emissions. 2009. Available online: https://www3.epa.gov/ttnchie1/conference/ei18/session6/andre.pdf (accessed on 19 July 2021).

57. André, M. The ARTEMIS European driving cycles for measuring car pollutant emissions. *Sci. Total Environ.* **2004**, *334–335*, 73–84. [CrossRef]

58. The MathWorks, Inc. Model-Based Calibration Toolbox. Available online: https://ww2.mathworks.cn/en/products/mbc.html (accessed on 19 April 2022).

59. Hartwich, F.; Beggiato, M.; Dettmann, A.; Krems, J. Drive Me Comfortable. Customized Automated Driving Styles for Younger and Older Drivers. In *Der Fahrer im 21. Jahrhundert: Fahrer, Fahrerunterstützung und Bedienbarkeit; Proceedings of the 8. VDI-Tagung, Braunschweig, Germany, 10–11 November 2015*; VDI-Verlag GmbH: Düsseldorf, Germany, 2015; pp. 271–283, ISBN 978-3-18-092264-5.